Available online at www.sciencedirect.com
SCIENCE DIRECT
Journal of Catalysis 234 (2005) 463–475
JOURNAL OF CATALYSIS
www.elsevier.com/locate/jcat

# Effect of pretreatment conditions on Cu/Zn/Zr-based catalysts for the steam reforming of methanol to $H_2$

Paul H. Matter, Umit S. Ozkan *

*The Ohio State University, Department of Chemical Engineering, 140 W. 19th Ave., Columbus, OH 43210, USA*

Received 31 March 2005; revised 4 July 2005; accepted 8 July 2005

Available online 11 August 2005

**Abstract**

A series of Cu/Zn/Zr-based catalysts for the methanol steam reforming reaction were found to have varying activity depending on composition and pretreatment conditions. The catalyst with a Cu:Zn:Zr mole ratio of 4:3:3 calcined at 350 °C performed equally well with or without prereduction in hydrogen, whereas catalysts containing alumina or calcined at 550 °C required prereduction with hydrogen for optimal activity. X-ray diffraction and thermogravimetric analysis showed that the bulk CuO phase of all of the catalysts is reduced to $Cu^0$ when reduced with hydrogen, methanol, or methanol and water. In addition, X-ray photoelectron spectroscopy shows that the most active sample without prereduction suffers the least amount of Cu surface composition loss during reduction with the steam reforming reactants, although differences in Cu surface composition cannot completely account for activity differences. Diffuse reflectance infrared Fourier transform spectroscopy experiments show that catalysts in their most active form have uniquely different spectra than the less active samples. For steam reforming over unreduced Cu:Zn:Zr 4:3:3 calcined at 350 °C, carbon dioxide bands eventually become the dominating feature, unlike for the other catalysts. Consequently, this is the only sample with a postreaction spectrum resembling the surface of its hydrogen-reduced counterpart. When steam reforming was carried out over the hydrogen-reduced surfaces, carbon dioxide was the dominating species observed for all samples, and the features that were apparent immediately after the hydrogen reduction remained intact. Several hypotheses are presented to explain these trends.


*Keywords:* Steam reforming of methanol; Cu–Zn catalysts; DRIFTS; XPS; TGA; DSC; Effect of prereduction of Cu

## 1. Introduction

Cu-based catalysts are potentially useful for several reactions, including low-temperature water–gas shift [1–3], methanol synthesis [4–11], and methanol reformation [12–18] and partial oxidation [19–22] to hydrogen. For these reactions, activity is generally proportional to Cu surface area and dispersion; therefore, the rate-determining steps for the various reactions are generally assumed to occur on Cu or at a boundary between Cu and the support [5,14,15,17,20,22–24]. Various oxides and mixtures of oxides can be used as supports for Cu, with the most common supports ZnO, $Al_2O_3$, $ZrO_2$, and mixtures of these oxides. Other promoters [24–26] and novel support structures with favorable effects also have been investigated [27].

From an academic standpoint, Cu-based catalysts are interesting due to the multiple functions of the supports. Zinc oxide is known to both improve the dispersion of Cu and the reducibility of CuO, and improved reducibility of CuO has been cited as a possible reason for the activity of Cu/ZnO catalysts if a Cu redox step occurs in the mechanism [16,28]. However, it is also possible that improved adsorption is a reason for the better activity and that improved reducibility is a second-hand effect. The adsorption properties of the support could affect activity, because spillover effects have been shown to play a role in reaction mechanisms for these catalysts. Hydrogen species are mobile over both phases of these catalysts and can be stored on the surface [6], whereas oxygen species have been shown to move from ZnO to Cu, most likely in the form of hydroxides [11].

* Corresponding author. Fax: +1-614-292-3769.
*E-mail address:* ozkan.1@osu.edu (U.S. Ozkan).

0021-9517/$ – see front matter 
doi:10.1016/j.jcat.2005.07.007

Like ZnO, zirconia improves the reducibility of copper and aids Cu dispersion [14,15,18,24]. Zirconia can also participate in spillover effects, because the buildup of hydrogen that spills over from Cu is possible on $ZrO_2$ as well [7,29,30]. For the methanol synthesis reaction, $ZrO_2$ has the attractive property of being able to adsorb $CO_2$, where it can become hydrogenated [7,31]. Likewise, for the steam reforming of methanol (SRM) reaction, $ZrO_2$ can readily adsorb methanol [32]. Moreover, higher-surface-area catalysts can be prepared through coprecipitation methods when both Zn and Zr are used together. Therefore, we have observed that it is favorable to use both ZnO and $ZrO_2$ together as a support for CuO to form catalysts with higher activity [17].

Alumina is generally added to the catalysts to improve surface area and prevent catalyst sintering [12,20]. However, excessive $Al_2O_3$ has an inhibiting effect on the SRM reaction in Cu/ZnO-based catalysts [14,17,20]. In addition, alumina does not improve the reducibility of CuO to the extent that ZnO or $ZrO_2$ does. The favorable effect of a small amount of alumina in reducing sintering generally outweighs the initial small loss of activity.

Limitations of these catalysts include the need for prereaction reduction, pyrophoricity, and questionable long-term stability. In previous work we demonstrated that unreduced zirconium-containing Cu/ZnO catalysts perform well for methanol reforming reactions even without prereaction reduction [17]. This is significant, because prereduction with hydrogen would be particularly burdensome for steam reforming systems used in mobile applications. It was apparent that the Cu component of the catalysts was at least partially reduced by the reactants; however, some catalysts, including alumina-containing samples and samples calcined at higher temperatures, still performed better after reduction with hydrogen. In addition, the extent of sample deactivation depended on composition and pretreatment conditions.

Other researchers have studied similar nonreduced Cu-based catalysts for methanol reforming reactions. Günter et al. examined the redox behavior of CuO/ZnO catalysts for methanol steam reforming using in situ X-ray diffraction (XRD) and X-ray absorption spectroscopy [33] and found that the bulk CuO phase is reduced under steam reforming conditions to metallic Cu. In addition, Cu/ZnO interactions had to be accounted for to explain activity observations. Specifically, activity was affected by increased disorder and microstrain in Cu particles, not just on the Cu surface area, caused by interaction with Zn. Likewise, Navarro et al. found that for the partial oxidation of methanol, reduction of CuO occurred under reaction conditions and led to active catalysts for hydrogen production [21]. Idem and Bakhshi examined oxidized Cu catalysts promoted with various elements for methanol steam reforming [26] and found that samples activated with the methanol and water reactant mixture were more active than the samples reduced with hydrogen. The methanol/water-activated samples contained a higher ratio of $Cu^+/Cu^0$ on the surface, just as the more active samples (for the various promoters studied) contained a higher $Cu^+/Cu^0$ ratio in postreaction analysis. This ratio was correlated with the stronger redox ability of Cu in these samples. Besides differences in Cu particle strain and redox ability (which may be related), differences in the Cu surface area after various additions of promoters and treatments also could contribute to activity differences. Thermal sintering leading to a loss of Cu surface area is widely known to be the primary cause of deactivation in these catalysts [23,34]. Varying promoters and pretreatments are also likely to affect Cu surface area through sintering differences.

In this paper we discuss how the catalyst surface interacts with methanol, describe the extent of catalyst reduction under steam reforming conditions, and explore the possible reasons for differences in activity among catalysts of varying composition and pretreatment conditions. A better understanding of the effects of such parameters will aid in the design of better catalysts and systems for methanol reforming to hydrogen in mobile systems that will not require catalyst prereduction with hydrogen.

## 2. Experimental

### 2.1. Catalyst preparation

The catalysts were prepared using a coprecipitation technique reported previously [17]. First, 1.25 mol solutions of Cu, Zn, and ZrO nitrates were mixed and then precipitated using 0.25 mol $Na_2CO_3$ under vigorous stirring at room temperature, with pH maintained at 8.5. The precipitate was then washed using suction filtration and 2 L of hot double-distilled water. The precursor was then dried overnight at 100 °C, crushed, and calcined. Calcination was carried out in a tube furnace using pure oxygen flowing at 10 sccm. The temperature was ramped from 25 °C to the maximum temperature at a rate of 5 °C/min. The maximum calcination temperature varied between 350 and 550 °C for different samples and was held there for 4 h. Surface area was determined by $N_2$ physisorption using a Micromeritics ASAP 2010 adsorption instrument.

### 2.2. Time-on-stream (TOS) activity testing

Activity testing was conducted in an in-house–constructed reactor system with an on-line HP5890 GC equipped with a thermal conductivity detector and a flame ionization detector (FID) for determining product composition. The FID was equipped with a methanizer to allow detection of CO at levels as low as 10 ppm. For all deactivation tests, 50 mg of the powder catalyst sample was loaded in a 5-mm-i.d., 316 stainless-steel tube. The reactor tube was then encased in an in-house-built furnace. A thermocouple measured the temperature at the bottom of the silica wool that supported the catalyst in the downward flow scheme. If the catalyst was prereduced, it was done in situ at 250 °C using 5% $H_2$ in $N_2$ flowing at 20 sccm for 3 h before activity testing. For all

steam reforming tests, the total flow rate was 100 sccm, with a composition of 15.5% methanol, 19.4% water, 36.9% $N_2$, and the balance Ar carrier. Measurements of product composition were made for up to 48 h TOS.

### 2.3. X-ray diffraction

Powder XRD patterns were obtained using a Bruker D8 X-ray diffractometer equipped with an HTK1200 sample holder capable of controlling temperature and atmosphere. The X-ray source was Cu–$K_\alpha$ radiation. For the $H_2$ reduction patterns, a fresh sample was placed in the sample holder; then, using a vacuum pump, the atmosphere was replaced with 5% $H_2$ in $N_2$. The temperature was then ramped under 10 sccm of 5% $H_2$ in $N_2$ flow, up to 250 °C at 5 °C/min and held for 1 h before measuring the pattern. For methanol reduction patterns, a fresh sample was placed in the holder, and the atmosphere was replaced with $N_2$ using a vacuum pump. The temperature was ramped to 250 °C at 5 °C/min under 10 sccm of $N_2$ flow. The temperature was held at 250 °C for 1 h, and then a pattern was obtained under $N_2$ flow. Next, 1% methanol flow in $N_2$ (10 sccm total) was initiated using a diffusion tube. Patterns were obtained after 1 and 2 h of methanol flow; these patterns were found to match each other for all of the samples tested. Water and methanol could not be sent to the instrument together because of the potential to produce an explosive mixture inside the instrument.

### 2.4. Thermogravimetric analysis/differential scanning calorimetry (TGA/DSC) with on-line gas chromatography mass spectroscopy (GC-MS)

Reduction of the catalysts with the reactants was examined using a Seteram TGA/DSC 111 connected to an on-line HP5890II GC/MS. For all tests, the instrument was placed in corrosive gas mode, and approximately 20 mg of sample was loaded onto the balance in a quartz crucible. For $H_2$ reduction experiments, the temperature was raised to 250 °C under He flow, and the balance was tared. Then 5% $H_2$ in $N_2$ was sent to the sample at 40 sccm while recording TGA and DSC signals for 1 h. Next, the same sample was held at 250 °C while purging with He flowing at 40 sccm for 1 h. Finally, approximately 1% methanol and 1.5% water in He (40 sccm total) was sent to the sample using diffusion tubes for 1 h to observe the effects of in situ steam reforming reaction with TGA, DSC, and MS signals. For nonreduced steam reforming experiments, a fresh sample was loaded into the instrument, and the temperature was raised to 250 °C under 40 sccm of He flow. Then 1% methanol and 1.5% water in He were sent to the sample while the TGA, DSC, and MS signals were recorded for 1 h. For methanol reduction experiments, a fresh sample was loaded into the instrument and the temperature was raised to 250 °C under He flow, then 1% methanol in He (40 sccm total) was sent to the sample for 1 h while recording TGA, DSC, and GC signals. The sample was then purged with He for 1 h while holding at 250 °C. Finally, the sample was reoxidized with 1.5% water in He flowing at 40 sccm for 18 h at 250 °C while performing TGA/DSC analysis. In all of the experiments, water was fed using a humidification bubbler, and methanol was fed using a diffusion tube. After each experiment, the flow was switched back to He to observe any changes in the baseline.

### 2.5. X-ray photoelectron spectroscopy (XPS)

X-ray photoelectron spectra were recorded using an AXIS Ultra XPS with an Mg anode operating at 14 kV and 10 mA. The powder sample was supported by double-sided carbon tape. For postreaction and postreduction experiments, the samples were sealed in He at the treatment temperature before being cooled, then loaded into the instrument without ever being exposed to the atmosphere by means of a glove box and a controlled-atmosphere transfer chamber. Charge shift corrections were made by assuming a C 1s binding energy of 284.5 eV for the carbon tape.

### 2.6. Diffuse reflectance infrared Fourier transform spectroscopy (DRIFTS)

The surface intermediates formed during in situ reductions and reactions were observed with a Bruker 1600 IR, equipped with a controlled-atmosphere sample holder. For all of the experiments in which a fresh sample was used, the surface was first cleaned by heating the sample in situ to 250 °C under He flow at 40 sccm for 1 h, and then a background spectrum was obtained at 250 °C under He flow. For the $H_2$-reduced sample, 5% $H_2$ in $N_2$ was sent to the sample at 20 sccm while holding the temperature at 250 °C for 1 h, but the spectra in He before the reduction was still used as the background. The $H_2$-reduced samples were then subjected to a reaction mixture of approximately 1% methanol and 1.5% water (using the same feed system as in the TGA experiments) in He flowing at 40 sccm. Spectra were taken every minute for 30 min, then every 5 min for the next 30 min. In one case additional spectra were taken every 30 min for 4 h. After the reaction was complete, the sample was flushed with He for 30 min, and then a final spectrum was taken at 250 °C. For nonreduced steam reforming experiments, a fresh sample was loaded, and, after taking a background, 1% methanol and 1.5% water in He with a total flow of 40 sccm was sent to the sample held at 250 °C. Similarly to the prereduced sample, spectra were taken every minute for 30 min, then every 5 min for the next 30 min, and after 1 h, the sample was flushed with He for 30 min and a final spectrum was taken at 250 °C. Methanol reduction experiments were also performed through an identical procedure, the only difference being the use of 1% methanol in He rather than water and methanol.

## 3. Results and discussion

### 3.1. TOS activity testing

Recently we reported differences in catalytic activity depending on reduction history and catalyst composition [17]. A $CuO/ZnO/ZrO_2$ catalyst with a mole ratio of 4:3:3, aptly named CZZ-433, performed quite differently in TOS tests depending on calcination temperature, prereduction with diluted $H_2$ at 250 °C, or the inclusion of alumina during preparation. When calcined at 350 °C, CZZ-433(350) was the best-performing SRM catalyst and performed equally well with or without prereduction, as shown in Fig. 1a. Here $H_2$ yield is defined as the mol of hydrogen produced divided by 3 times the mol of methanol fed, because the stoichiometry of the steam reforming reaction is 3 mol of hydrogen per mol of methanol. However, as reported previously, when calcined at 550 °C, the zirconia phase changed from an amorphous carbonate-containing phase to tetragonal, accompanied by a loss in surface area. CZZ-433(550) did not perform as well as its 350 °C counterpart for the SRM reaction without prereduction, but a temporary two-fold increase could be obtained with a reduction in diluted hydrogen, as shown in Fig. 1b. But this increased activity did not last, and after 20 h TOS, the catalyst performance deteriorated to the same level observed for the sample that was not prereduced. Interestingly, when a small amount of alumina was added to CZZ-433(350) a completely different trend was observed. Adding 5% alumina to the same ratio of components (named CZZA-433:0.5) resulted in a catalyst that required prereduction with $H_2$ to obtain an optimal activity that is maintained over time. Fig. 1c shows the trend seen for the alumina-containing catalyst. We have observed that this dependence on reduction with hydrogen for optimal activity is common for $Cu/ZnO/Al_2O_3$ commercial catalysts as well (data not shown).

### 3.2. XRD

For Cu-based catalysts, using harsher reduction conditions (e.g., a faster ramp rate or more concentrated hydrogen) is unadvisable, because this can decrease catalytic activity due to sintering and loss of Cu surface area. Therefore, we compared the sintering effects of different reduction treatments by obtaining XRD patterns during in situ reductions. Interestingly, all of the samples had to be recalcined before performing the experiments because of the apparent reactivity of CuO at atmospheric conditions. Several months after preparation, we observed that CuO peaks eventually vanish from the XRD patterns, whereas no new phase was apparent and the other metal oxides remained unaffected. A possible explanation for this finding could be the reaction of CuO with atmospheric water and carbon dioxide to form an amorphous hydroxy-carbonate, which was partially the form of the catalyst precursor. This process, known as the memory effect, is commonly observed for calcined double-layered

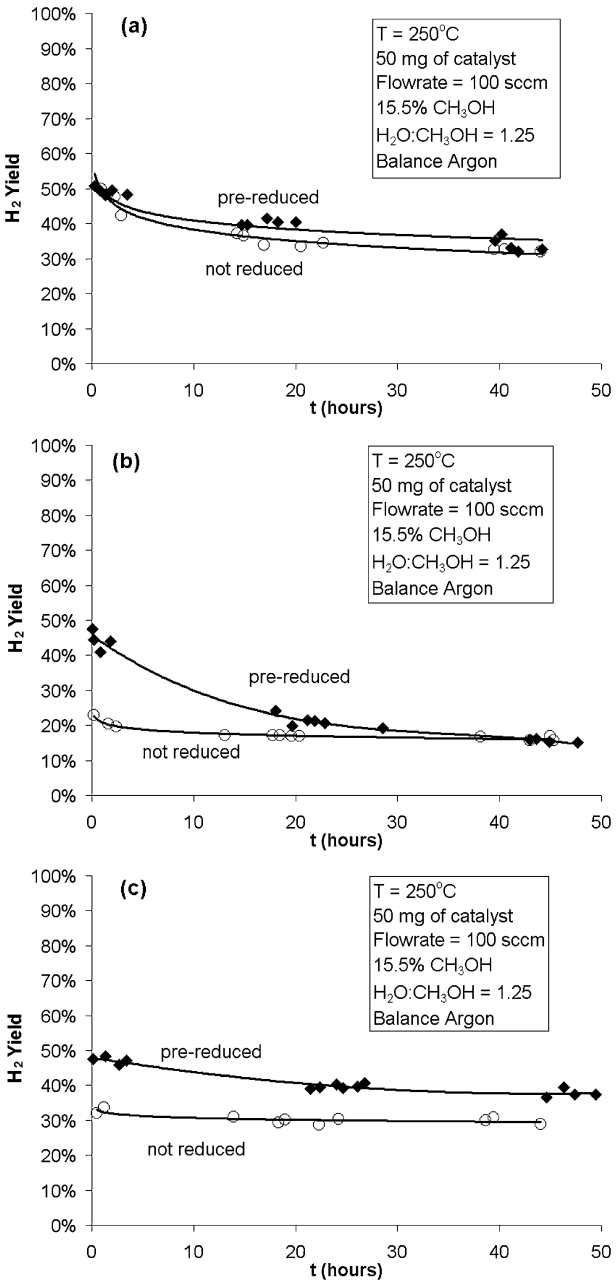


Fig. 1. Time-on-stream activity testing with and without prereduction by hydrogen for (a) CZZ-433(350), (b) CZZ-433(550), and (c) CZZA-433:0.5.

hydroxides that have been exposed to water and carbon dioxide or aqueous carbonate solutions [35]. Recalcining the samples in oxygen returned them to their initial crystalline form. The three samples examined were CZZ-433(350), CZZ-433(550), and CZZA-433:0.5. Fig. 2 shows the in situ XRD patterns of samples after calcination, after reduction in 5% $H_2$ in $N_2$ at 250 °C, and after reduction in 1% methanol at 250 °C. The samples all look similar, with the exception of the higher crystallinity and the presence of the tetragonal zirconia phase in the sample calcined at 550 °C. Methanol, like hydrogen, was able to reduce the bulk CuO to $Cu^0$ completely in all of the samples. The higher intensity and the

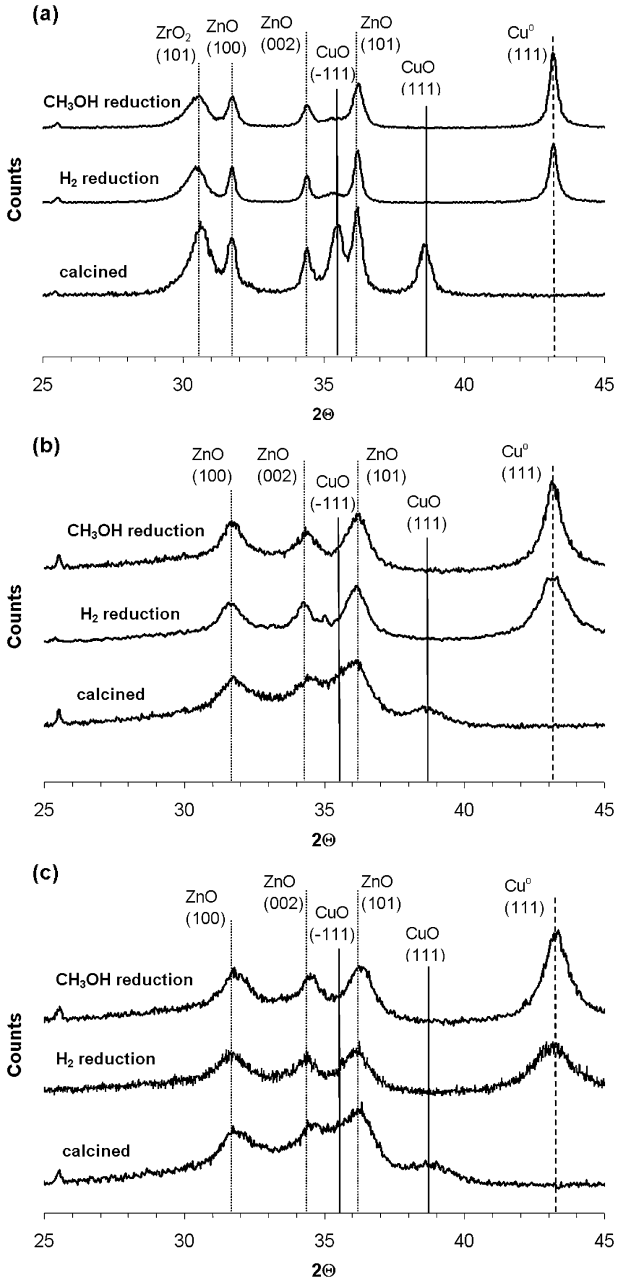


Fig. 2. XRD patterns after various in situ treatments for (a) CZZ-433(550), (b) CZZ-433(350), and (c) CZZA-433:0.5.

narrower width of the $Cu^0$ (111) diffraction line observed over the methanol-reduced samples clearly shows that $Cu^0$ sinters more easily when reduced with methanol than when reduced with hydrogen. There are two possible explanations for the increased sintering seen when using methanol as a reductant. First, pure methanol could be causing a chemical effect, such as leading to the formation of Cu carbonyl species that facilitate faster sintering of the Cu. A second possibility is a thermal effect in which more heat is released when using methanol as the reductant compared to hydrogen (see Section 3.2). It should be pointed out that the methanol was not sent to the sample until the temperature reached

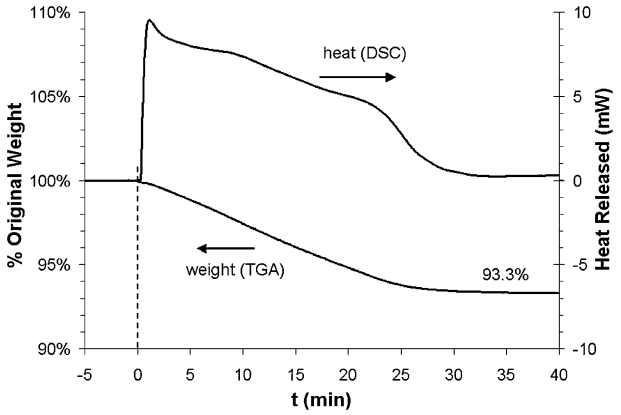


Fig. 3. TGA/DSC signals for the reduction of CZZ-433(550) with 5% $H_2$ in $N_2$ at 250 °C.

250 °C, whereas 5% $H_2$ in $N_2$ was sent to the sample during the temperature ramping. This was done to mimic the TOS activity testing procedure and may have aided sintering during the reduction with methanol. However, for activity testing, a methanol concentration of 15% (not 1%) was used, so the sintering may have been even worse for the nonreduced samples tested with TOS, assuming that the presence of water does not have a significant effect on the sintering process. Unfortunately, higher methanol concentrations and water together with methanol could not be sent to the XRD sample chamber, because of safety concerns. Nonetheless, these experiments show that it is possible for methanol to completely reduce the bulk CuO phase and to sinter the particles in the process even more so than hydrogen.

### 3.3. TGA/DSC with online GC-MS

Several experiments were carried out with the TGA/DSC setup to better characterize the reduction process of the catalysts. All of the catalysts showed similar trends; therefore, only the results for one of the catalysts, CZZ-433(550), is presented in graphical form here. This was the catalyst with the largest activity disparity for the nonreduced sample. Any observed differences between samples are noted in the discussion and also reported in Table 1.

In the first experiment, the catalysts were reduced with 5% $H_2$ in $N_2$ at 250 °C. The DSC signal shows that the reduction of CZZ-433(550) was fairly fast and exothermic (Fig. 3). The total weight loss from the original weight during the reduction was 6.7%. If it were assumed that the only cause of weight change is the reduction of CuO to Cu, then, based on the "as prepared" composition, a weight loss of 6.8% would be expected, thus matching the measured value within the error of the measurement. The other samples tested, CZZ-433(350) and CZZA-433:0.5, had weight reductions of 7.2 and 6.7%, respectively, as shown in Table 1. To obtain the heat of reduction in Table 1, the exotherm was integrated and then divided by the amount of CuO in the sample. At 250 °C and atmospheric pressure, the reduction of CuO with hydrogen is expected to be exothermic with a

Table 1
Overview of reduction experiments with TGA/DSC

| Sample | Reducion atmosphere | Temperature (°C) | Weight lost | Heat released (kJ/mol Cu) | Note |
|---|---|---|---|---|---|
| CZZ-433(550) | $H_2$ | 250 | 6.7% | 74.3 | See Fig. 3 |
| CZZ-433(550) | $H_2$ | ramped | 6.7% | 72.8 | Not shown |
| CZZ-433(550) | MeOH and $H_2O$ | 250 | 6.4% | 60.3 | See Fig. 5 |
| CZZ-433(550) | MeOH | 250 | 6.6% | 69.5 | See Fig. 6 |
| CZZ-433(350) | $H_2$ | 250 | 7.2% | 64.2 | Not shown |
| CZZ-433(350) | MeOH and $H_2O$ | 250 | 6.9% | 56.0 | Not shown |
| CZZ-433(350) | MeOH | 250 | 7.2% | 59.7 | Not shown |
| CZZA-433:0.5 | $H_2$ | 250 | 6.7% | 73.7 | Not shown |
| CZZA-433:0.5 | MeOH and $H_2O$ | 250 | 6.3% | 62.0 | Not shown |
| CZZA-433:0.5 | MeOH | 250 | 6.5% | 63.5 | Not shown |

heat of reaction slightly more negative than the experimental values:

$$CuO + H_2 \rightarrow Cu^0 + H_2O \quad \Delta H \text{ at } 250\,^{\circ}C = -85\ \text{kJ/mol}.$$

The endothermic decomposition of hydroxy-carbonates during the reduction, as seen previously for the decomposition of the precursor [17], could account for the lower than expected heat of reduction seen in all of the samples. These samples were calcined ex situ to mimic the procedure used for activity testing; therefore, some hydroxycarbonates that can form on exposure to the atmosphere and decompose above 250 °C could still have been present. Carbon dioxide formation observed during catalyst reduction with hydrogen lends further support to this possibility. This observation is discussed further in Section 3.4. Interestingly, CZZ-433(350) lost slightly more weight than the other samples and exhibited the least heat release during reduction, suggesting that it might contain more hydroxy-carbonates than the other samples.

The reduction was also carried out for CZZ-433(550) while ramping the temperature at 5 °C/min from 25 °C up to 300 °C (data curves not shown). As shown in Table 1, the same amount of weight was lost, and only 1.5 kJ/mol less heat was released; however, it is more difficult to obtain a baseline for the DSC signal in the ramping experiment, and thus only constant temperature reductions were carried out for all of the samples.

Next, the SRM reaction was carried out over the hydrogen-reduced catalysts. The reaction seemed to reach steady state very quickly for all catalysts, as shown in Fig. 4 for CZZ-433(550). The reaction products and unreacted feed detected with the GC-MS reached a steady level after 5 min (not shown). The DSC signal dropped to an endothermic value for all samples because the endothermic steam reforming reaction took place on the sample. The weight of the samples increased only slightly (<0.5%) and remained steady for the duration of the 1-h-long experiment for all samples. This slight weight increase may be caused by intermediates present on the surface. After the reaction, the sample was flushed with helium, and the DSC curve returned to the original baseline, whereas the weight remained slightly

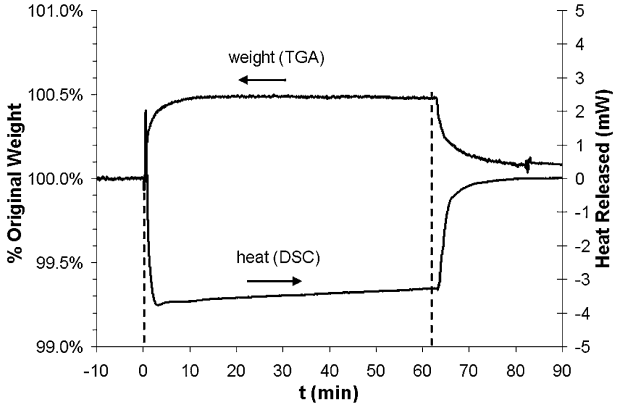


Fig. 4. TGA/DSC signals for the in situ steam reforming of methanol over prereduced CZZ-433(550) at 250 °C.

higher than the original baseline (about 0.1% for all samples). This could be due to partial reoxidation of the surface during SRM reaction or to some intermediates remaining on the surface.

The steam reforming reaction was also carried out in the TGA/DSC system over the unreduced sample. The results of this experiment for CZZ-433(550) are shown in Fig. 5a, and the values for weight loss and heat released for all samples are reported in Table 1. The reduction of the bulk of the catalyst seen on XRD with methanol alone as the reducing agent occurs even in the presence of water. The TGA signal shows a catalyst weight loss of 6.4%, similar to the weight loss for the reduction with $H_2$. The DSC signal is also similar to the $H_2$ reduction signal, but falls to an endothermic baseline rather than to zero. This is because the endothermic steam reforming reaction begins to occur after CuO is reduced. Overall, this reduction occurred faster but was less exothermic than hydrogen reduction. The other samples had the same trend and shape for the TGA and DSC signals. The products from the reaction, reported by the GC-MS analysis in Fig. 5b, shows that more $CO_2$ and $H_2O$ is being released when the sample is still losing mass, but that the $CO_2$ and $H_2O$ concentrations level out once the mass change subsides. Copper oxide is known to catalyze the full oxidation of methanol to water and carbon dioxide [16,36],

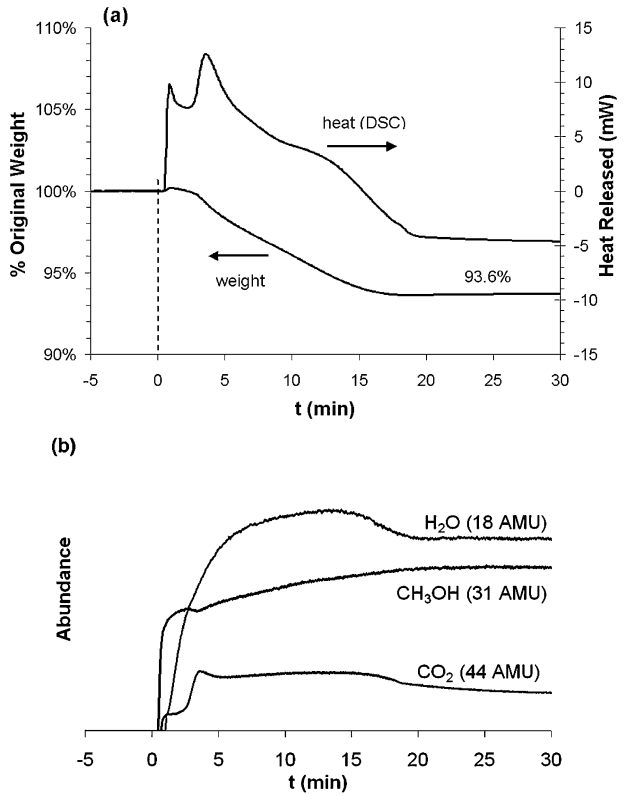


Fig. 5. Steam reforming of methanol over nonreduced CZZ-433(550) at 250 °C, (a) TGA/DSC signals for in situ reaction, and (b) abundance of the products from the experiment detected with on-line mass spectrometer.

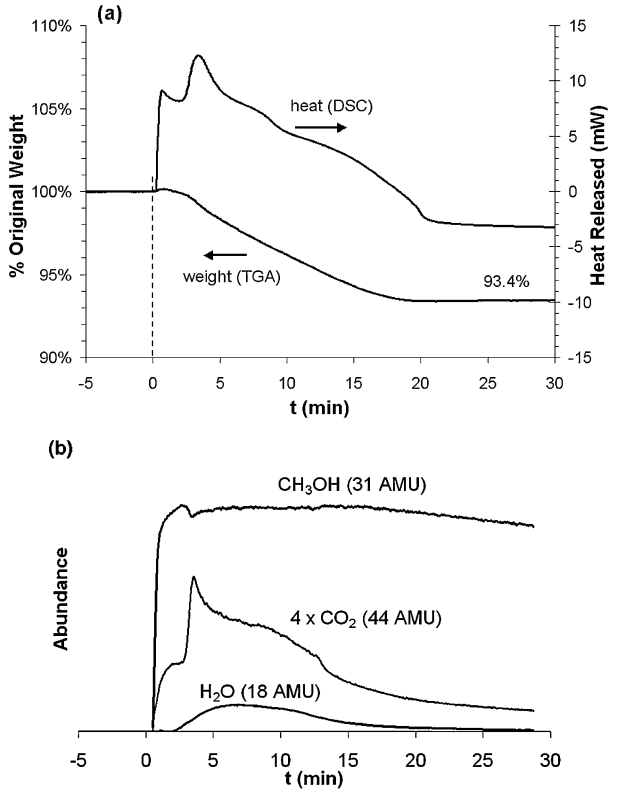


Fig. 6. Reduction of CZZ-433(550) with methanol at 250 °C, (a) TGA/DSC signals for in situ reduction, and (b) abundance of the products from the experiment detected with on-line mass spectrometer.

with the reaction likely depleting the oxygen of the catalyst by the following reaction:

$$\mathrm{CuO} + (1/3)\mathrm{CH_3OH} \rightarrow \mathrm{Cu^0} + (1/3)\mathrm{CO_2} + (2/3)\mathrm{H_2O}$$

$$\Delta H \text{ at } 250\,^{\circ}\mathrm{C} = -60\ \mathrm{kJ/mol}.$$

Per mol of CuO, this reaction is less exothermic than the reduction of CuO with hydrogen. The corresponding values from the integration of the DSC signal agree. However, sintering may cause a higher heat of reduction in some of the samples, whereas carbonate/hydroxide decomposition could lower the heat of reduction. Coincidentally, the sample that is most active after reduction with the reactants, CZZ-433(350), was the sample with the least amount of heat released during the reduction.

During reduction with methanol only, the reaction to $CO_2$ and $H_2O$ is even more obvious. The DSC signal (shown in Fig. 6a) is nearly the same as for steam reforming over a nonreduced sample, although the final baseline is less endothermic. Integration of the DSC curve indicates a more exothermic heat of reduction for the methanol reduction compared with the reduction where water is also present. Fig. 6b shows that $CO_2$ and $H_2O$ are released only until the weight loss ceases. These trends held true for all three samples tested. With respect to the endothermic baseline, in TOS activity testing, the amount of CO produced was <700 ppm, with a selectivity of $CO_2$ compared to CO of 99.8%. Even in preliminary reaction experiments where pure methanol was sent to a reduced catalyst, the conversion of methanol to CO was <1%, so it is unlikely that the endothermic baseline stems from the decomposition of methanol. It is difficult to detect such a small amount of CO with MS considering the fact that methanol, carbon dioxide, and even $N_2$ contamination have mass fragments at 28 AMU. The slightly endothermic baseline in this case may result in large part from an imperfect flow balance between the reference and sample side, rather than from methanol decomposition. In cases where the steam reforming reaction can occur, the endothermic baseline (which is even lower) is likely coming from both the endothermic steam reforming reaction and flow differences.

After 1 h, the methanol-reduced sample was purged with He, and then an attempt was made to reoxidize the samples with water vapor at 250 °C (Fig. 7). Initially, the DSC signal indicated an exothermic spike, perhaps from reaction of leftover surface species (although valve changes can cause experimental error in the signal). Then the weight of the sample began to increase slowly over the next 18 h. The final weight of the sample indicated it was about 50% reoxidized; however, examination of the sample after its removal from the instrument showed that the top layer was yellowish/green in color and the bottom layer was black, indicating that the 50% oxidation may have been from uneven oxidation of the sample, not necessarily from oxidation to $Cu^+$. The weight of the other methanol-reduced samples slowly increased af-

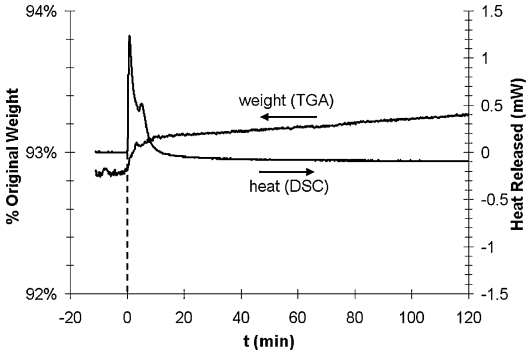


Fig. 7. TGA/DSC signals for the re-oxidation of methanol reduced CZZ-433(550) with water at 250 °C.

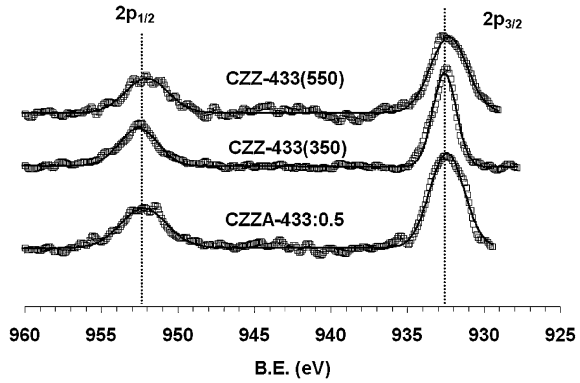


Fig. 8. Cu 2p XPS spectra of samples after reduction with methanol.

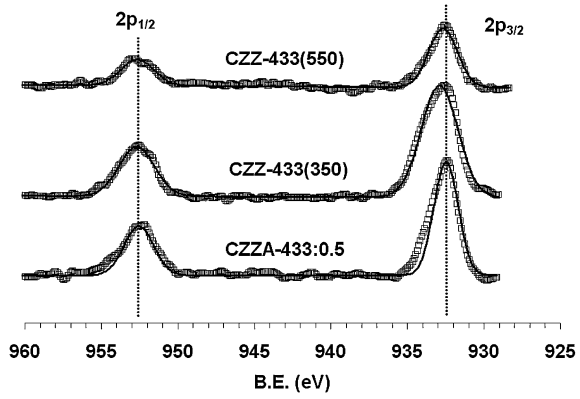


Fig. 9. Cu 2p XPS spectra of samples after reduction with the methanol and water reactant mixture.

ter water was added in the same manner. It has been reported that the oxidation of $Cu^0$ to $Cu^+$ could be part of the reaction mechanism in steam reforming, water–gas shift, and methanol synthesis [26,28,33]. Evidently, these experiments demonstrate that reoxidation of the bulk Cu with water is extremely slow compared with the reduction of CuO.

### 3.4. XPS

Although XRD and TGA results agree that the bulk CuO phase of the catalysts is fully reduced, these techniques do not give any indication of the extent of reduction on the surface. In addition, the same treatment conditions used for activity testing cannot be used for these techniques because of instrument limitations. Therefore, XPS analysis was performed on all three catalysts after three different treatments. In the first treatment, the catalysts were reduced with 5% $H_2$ in $N_2$ while ramping the temperature by 5 °C/min up to 250 °C; in the second treatment, the catalysts were reduced with 15.5% methanol in He while holding the temperature at 250 °C; and in the third treatment, the catalysts were reduced with 15.5% methanol and 19.4% water in He at 250 °C. These conditions were identical to the conditions used for TOS activity testing. The results of this analysis in terms of metal compositions on the surface and binding energies are presented in Table 2, with results from the calcined catalysts also given for comparison. The trends in activity testing show some correlation to the copper surface concentration measured by XPS. When the catalysts are carefully reduced with $H_2$, the Cu surface area decreases slightly on a metal basis, with the exception of the alumina-containing sample, which remains about the same. Alumina is known to reduce sintering of Cu during the reduction process because of a strong interaction between Cu and surface Al [37]. However, the reduction of the catalysts in methanol cuts the Cu surface composition at least in half for all samples. Reduction of the catalysts with water and methanol was not as harsh as that with methanol only, but the total Cu surface composition was still less than that seen after hydrogen reduction. The catalyst calcined at 350 °C seemed to fare the best after reduction with the reactants in terms of both Cu surface composition and activity. In contrast, the differences in Cu surface composition between the various reduction methods for the samples alone do not appear sufficiently extreme to account for the observed differences in activity.

The Cu 2p regions for samples reduced by methanol (Fig. 8) and samples reduced by the reaction mixture (Fig. 9) were fit to a single peak. For all of the samples, the binding energy of this peak was close to or slightly higher than the binding energy for the corresponding sample reduced with hydrogen. It is possible to fit the peaks in Figs. 8 and 9 with a shoulder with higher binding energy, as was done by Agrell et al. [16] for similar samples after exposure to a methanol and oxygen mixture. It is also possible that there are $Cu^+$ species on the surface, because binding energies for these species typically overlap with those for $Cu^0$ species in Cu 2p XPS analysis. A detailed analysis of the Cu LMM region (not performed), is needed to differentiate between $Cu^0$ and $Cu^+$. Other researchers who analyzed the Auger electron spectra detected both oxidation states of Cu in reduced catalysts [38–40]. In their analysis of hydrogen-reduced Cu/ZnO methanol synthesis catalysts, Okamoto et al. attributed the $Cu^0$ phase to larger metallic $Cu^0$ crystallites, and assigned the $Cu^+$ phase to a two-dimensional Cu phase on ZnO that is derived from Cu dissolved in the ZnO lattice [38]. This may explain the slightly higher binding energies of some of the samples and the possible shoulders with higher binding

Table 2
Overview of post reduction XPS analysis

| Sample | Treatment | Region | BE (eV) | Metal surface coverage | Surface coverage |
|---|---|---|---|---|---|
| CZZ-433(550) | Calcined | Cu $2p_{3/2}$ | 933.6 | 18.1% | 5.1% |
| | | Zn $2p_{3/2}$ | 1022.2 | 56.6% | 16.1% |
| | | Zr $3d_{5/2}$ | 181.9 | 25.3% | 7.2% |
| | $H_2$ | Cu $2p_{3/2}$ | 932.3 | 13.3% | 6.2% |
| | | Zn $2p_{3/2}$ | 1022.2 | 63.2% | 29.6% |
| | | Zr $3d_{5/2}$ | 182.5 | 23.6% | 11.0% |
| | $CH_3OH$ | Cu $2p_{3/2}$ | 932.3 | 6.1% | 2.8% |
| | | Zn $2p_{3/2}$ | 1022.3 | 55.8% | 25.9% |
| | | Zr $3d_{5/2}$ | 183.4 | 38.2% | 17.7% |
| | $CH_3OH + H_2O$ | Cu $2p_{3/2}$ | 932.7 | 12.5% | 4.9% |
| | | Zn $2p_{3/2}$ | 1022.4 | 65.8% | 25.9% |
| | | Zr $3d_{5/2}$ | 182.3 | 21.8% | 8.6% |
| CZZ-433(350) | Calcined | Cu $2p_{3/2}$ | 933.7 | 25.7% | 7.0% |
| | | Zn $2p_{3/2}$ | 1022.1 | 53.3% | 14.6% |
| | | Zr $3d_{5/2}$ | 181.7 | 20.9% | 5.7% |
| | $H_2$ | Cu $2p_{3/2}$ | 932.5 | 17.5% | 6.5% |
| | | Zn $2p_{3/2}$ | 1022.0 | 70.1% | 26.0% |
| | | Zr $3d_{5/2}$ | 183.0 | 12.5% | 4.6% |
| | $CH_3OH$ | Cu $2p_{3/2}$ | 932.6 | 8.0% | 3.9% |
| | | Zn $2p_{3/2}$ | 1022.0 | 79.2% | 38.7% |
| | | Zr $3d_{5/2}$ | 182.9 | 12.9% | 6.3% |
| | $CH_3OH + H_2O$ | Cu $2p_{3/2}$ | 932.7 | 16.6% | 7.2% |
| | | Zn $2p_{3/2}$ | 1022.4 | 74.7% | 32.3% |
| | | Zr $3d_{5/2}$ | 183.2 | 8.6% | 3.7% |
| CZZA-433:0.5 | Calcined | Cu $2p_{3/2}$ | 933.5 | 12.6% | 5.2% |
| | | Zn $2p_{3/2}$ | 1022.0 | 32.3% | 13.2% |
| | | Zr $3d_{5/2}$ | 181.7 | 13.6% | 5.6% |
| | | Al 2p | 76.9 | 41.5% | 7.5% |
| | $H_2$ | Cu $2p_{3/2}$ | 932.5 | 12.8% | 6.9% |
| | | Zn $2p_{3/2}$ | 1022.0 | 38.7% | 20.7% |
| | | Zr $3d_{5/2}$ | 183.0 | 11.2% | 6.0% |
| | | Al 2p | 75.4 | 37.2% | 19.9% |
| | $CH_3OH$ | Cu $2p_{3/2}$ | 932.5 | 5.8% | 3.1% |
| | | Zn $2p_{3/2}$ | 1022.0 | 55.9% | 29.6% |
| | | Zr $3d_{5/2}$ | 183.8 | 14.6% | 7.7% |
| | | Al 2p | 76.3 | 23.6% | 9.0% |
| | $CH_3OH + H_2O$ | Cu $2p_{3/2}$ | 932.5 | 10.1% | 5.0% |
| | | Zn $2p_{3/2}$ | 1022.4 | 54.9% | 26.7% |
| | | Zr $3d_{5/2}$ | 182.5 | 9.3% | 4.5% |
| | | Al 2p | 75.3 | 25.6% | 10.7% |

energy. However, based on the absence of satellite peaks in the Cu 2p region, it can be definitively concluded that there are no $Cu^{2+}$ species on the surface.

Generally, the surface coverage of Zn increased after reduction of CuO with any choice of reactant (see Table 2). Although the binding energies changed only slightly, they were consistently higher after reduction with the reactants. This trend also holds for postreaction samples subjected to prereduction with hydrogen [17]. The Zn 2p region of CZZ-433(550) after various treatments is shown in Fig. 10; in each case, one peak provided a reasonable fit.

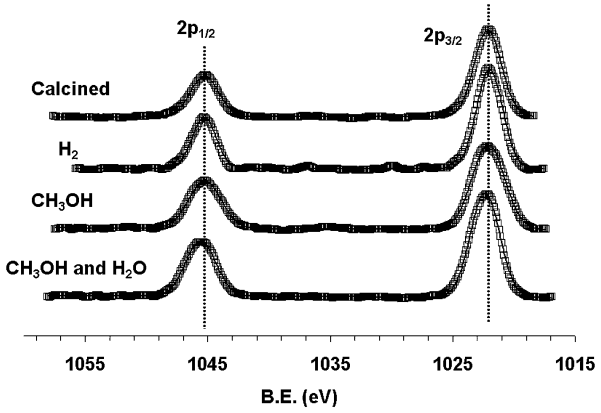


Fig. 10. XPS spectra of Zn 2p region for CZZ-433(550) after various pretreatments.

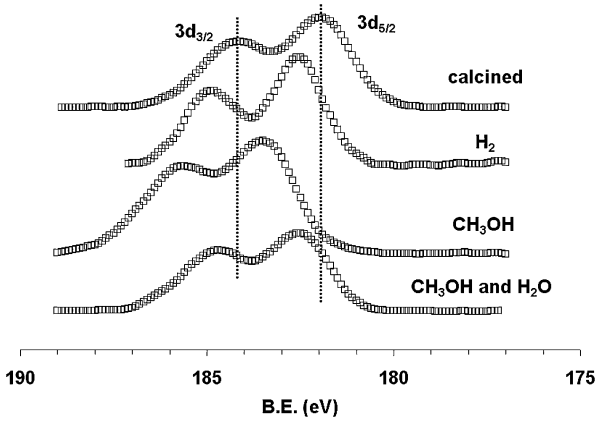


Fig. 11. XPS spectra of Zr 3d region for CZZ-433(550) after various pretreatments.

There was no consistent trend in terms of Zr surface composition of the catalysts. Interestingly, however, the binding energy of the Zr 3d electron increased after reduction in any atmosphere for all of the samples. Fig. 11 shows the Zr 3d XPS spectra for CZZ-433(550). Others have used a two-peak deconvolution to fit to the Zr 3d region in similar oxidized catalysts [41]. The reduced samples have spectra similar in shape to the oxidized sample; however, the hydrogen-reduced sample has the sharpest peaks. It is possible that various surface species are creating the broader spectra in the other samples. As discussed earlier (see Section 1), the adsorption of methanol and carbon dioxide on zirconia could lead to changes in the electron density surrounding Zr atoms.

For CZZA-433:0.5, a disproportionately large amount of alumina was found on the surface. Extensive enrichment of the surface with alumina has been reported for samples containing even less alumina as well [16,37]. The alumina surface composition and binding energy decreased with reduction of CuO. There was no evidence of copper aluminate (in the Cu or Al spectra) on XPS, although others have detected this component by other means in similar catalysts [24,37]. The Al 2p spectrum (not shown) is partially overlapped by the Cu 3p peak; therefore, deconvolution was nec-

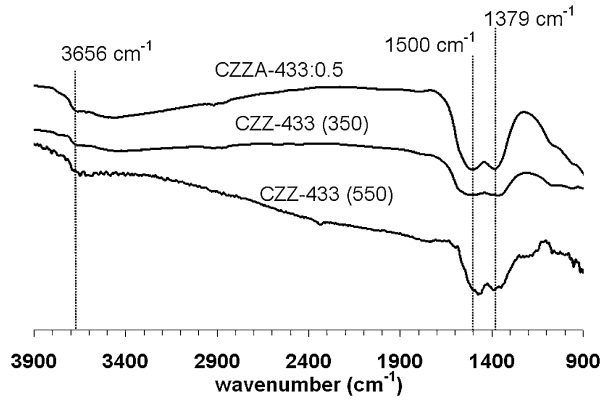


Fig. 12. DRIFTS spectra of samples after reduction with hydrogen at 250 °C.

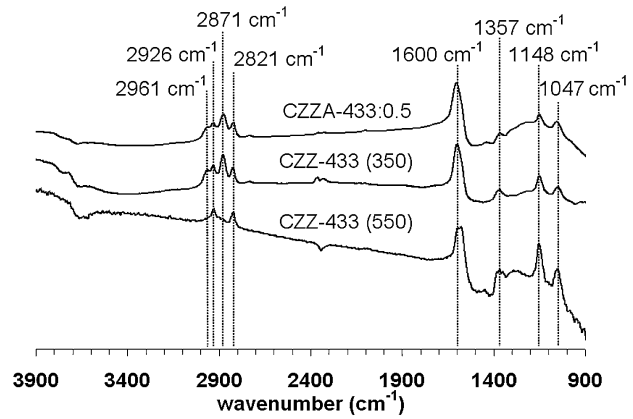


Fig. 13. DRIFTS spectra of samples after reduction with methanol at 250 °C.

essary to obtain a rough quantitative measure of the alumina peak area.

### 3.5. DRIFTS

The surface reactions occurring over these catalysts during reduction and reaction can be analyzed with DRIFTS to provide more details about the catalyst surfaces during various treatments. Limited work has been performed to study the methanol reforming reactions using this technique [13,42]; however, significant work has been done to study methanol synthesis on Cu-based catalysts [7,30–32,43–48]. This has aided the development of mechanistic models for steam reforming, the reverse of the methanol synthesis reaction. The experiments run on the samples while recording DRIFTS spectra mirrored the experiments run with the other characterization techniques in this study, to allow for comparison of results.

In the first experiment, the catalysts were reduced with hydrogen to observe the changes occurring in the infrared spectrum of the surface. The results obtained after flushing with He are shown in Fig. 12. The reduction caused broad valleys in the spectra near 1500 and 1379 $cm^{-1}$. These valleys are likely from the loss of leftover carbonate species from the precipitation that were not removed during calcination. It is also possible that such species formed from exposure to $CO_2$ in the atmosphere. Monodentate carbonate is known to have bands consistent with the valleys observed and has been reported to be a stable species on similar materials [45,48,49]. Although copper–oxygen bonds are also expected to disappear during the reduction, these bands are not expected to be in this region [50]. Carbon dioxide peaks at 2359 and 2327 $cm^{-1}$ (not shown) were observed in the early stages of sample reduction, providing evidence that a carbon species was being reduced. Some loss of hydroxide species was also apparent in the spectra, with a consistent valley at 3656 $cm^{-1}$. At higher wave numbers, however, there was an apparent increase in intensity, which may indicate changes in the hydroxide region due to water formation.

Table 3
Surface species identified by DRIFTS

| Species | Formula | Vibration | Wavenumber ($cm^{-1}$) |
|---|---|---|---|
| Methoxy | M–$OCH_3$ | $\nu$(C–O) | 1047 |
| | | $\nu(C–H)_s$ | 2821 |
| | | $\nu(C–H)_a$ | 2926 |
| Bridging methoxy | $M_2$–$OCH_3$ | $\nu$(C–O) | 1148 |
| Formaldehyde | $\pi$-bonded $CH_2O$ | $\nu$(C–O) | 1148 |
| Formate | M–OOCH | $\nu(C–O)_s$ | 1357 |
| | | $\nu(C–O)_a$ | 1600 |
| | | $\nu$(C–H) | 2871 |
| | | $\nu$(C–H) | 2961 |

Reduction with methanol was shown to have the same effect as reduction with hydrogen by XRD, TGA, and XPS, although methanol seemed to sinter the catalysts more. However, the DRIFTS spectra in Fig. 13 show that the infrared spectra of the methanol-treated surfaces differed from the postreduction with hydrogen spectra. The valleys at 3656, 1500, and 1379 $cm^{-1}$ were still present, but leftover species from the reduction remained on the surface even after the He flushing. The bands for these species match the bands for intermediate species often reported for the methanol synthesis and steam reforming reactions [13,42]. Table 3 reports the identified stable intermediate species along with their band assignments. The first step in steam reforming is thought to be the adsorption of methanol to form a methoxy group. A plausible route for methoxy formation is the reaction of methanol with hydroxyl surface groups to form water and methoxy. The valleys in the hydroxyl region are consistent with this route. Duprez et al. observed methanol adsorption on zirconia through this mechanism, and other metal oxides likely could adsorb methanol in a similar manner [32]. It is also possible for methanol to adsorb onto Cu and Cu oxide surfaces, leading to the formation of methoxy groups [51–54]. Methoxy C–O stretching was observed at 1047 $cm^{-1}$, and the C–H stretching bands were seen at 2821 $cm^{-1}$ (symmetric) and 2926 $cm^{-1}$ (asymmetric) on all the samples. After removal of a hydrogen atom, the methoxy

species can form formaldehyde, and the band at 1148 $cm^{-1}$ may be due to formaldehyde; however, this band has also been assigned to a bridging methoxy species [55]. Furthermore, formaldehyde is not expected to be very strongly bonded to copper, and it generally reacts quickly at this temperature over Cu-based materials, whereas methoxy is known to be more stable [45,47,54]. However, several earlier studies have attributed this band to $\pi$-bonded formaldehyde [13,48], and both possible species have C–H stretching bands near the methoxy C–H bands, so neither possibility can be absolutely ruled out. Before forming $CO_2$, the reactants are believed to pass through a formate intermediate. Formate bands were apparent at 1357, 1600, 2871, and 2961 $cm^{-1}$. The formate band at 1357 $cm^{-1}$ partially covers the valley believed to be from the removal of carbonates. Methanol synthesis work has suggested that these species are present on the zirconia or zinc oxide phases. However, because copper was oxidized before the introduction of methanol, these species could be present on Cu as well. In an earlier study, Wachs and Madix showed that methanol adsorbs onto oxidized copper and decomposes to formaldehyde and formate while reducing Cu at the same time [54].

In the next series of experiments, methanol and water were sent to the oxidized catalysts at 250 °C. This series of experiments involved significant differences between the samples, unlike in the previous experiments. The same intermediate species that were left over from methanol reduction can be seen on the samples during methanol steam reforming, with the methoxy species having a stronger presence during the steam reforming, as shown in Figs. 14a–14c. In addition, gas phase or weakly adsorbed carbon dioxide bands are observed at 2327 and 2359 $cm^{-1}$. After flushing with helium, the intermediate bands subside and the carbon dioxide bands disappear, although the apparently more stable formate bands remain on the alumina-containing sample, as shown in Fig. 15. The postreduction spectra also show that after reduction with the reactants, two of the catalysts do not have large valleys in the carbonate region. However, a valley for CZZ-433(350) does seem to be starting to form. Interestingly, this catalyst also had an apparent abundance of hydroxides above the 3656 $cm^{-1}$ valley that was not present for the other samples after reduction with methanol or methanol and water, but was present for all samples after reduction with hydrogen.

Additional features in the FTIR spectra are worth noting when the sample is reduced with methanol and water (Fig. 14). Interestingly, the alumina-containing sample has a unique band at 2095 $cm^{-1}$, believed to belong to adsorbed carbon monoxide. However, the most interesting difference between the samples is the fact that the intermediates, with the exception of $CO_2$, decline after 30 min on CZZ-433(350) but remain steady on the other two samples. During actual reaction experiments, the concentrations of methanol and water are higher, so these transitions likely occurred more quickly (before the first product sampling) in the activity ex-

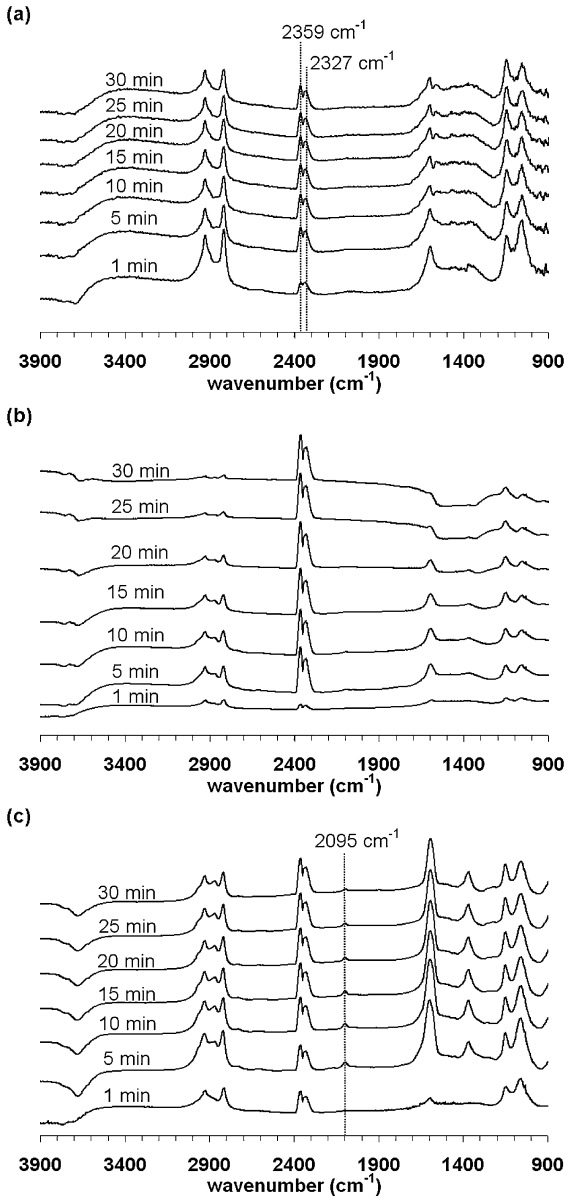


Fig. 14. DRIFTS spectra of in situ steam reforming of methanol over nonreduced samples (a) CZZ-433(550), (b) CZZ-433(350), and (c) CZZA-433:0.5.

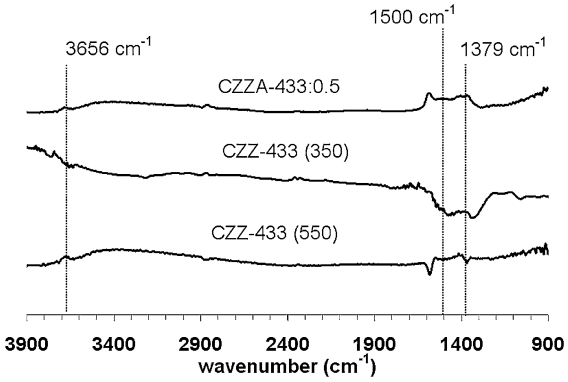


Fig. 15. DRIFTS spectra of samples after reduction with methanol and water at 250 °C.

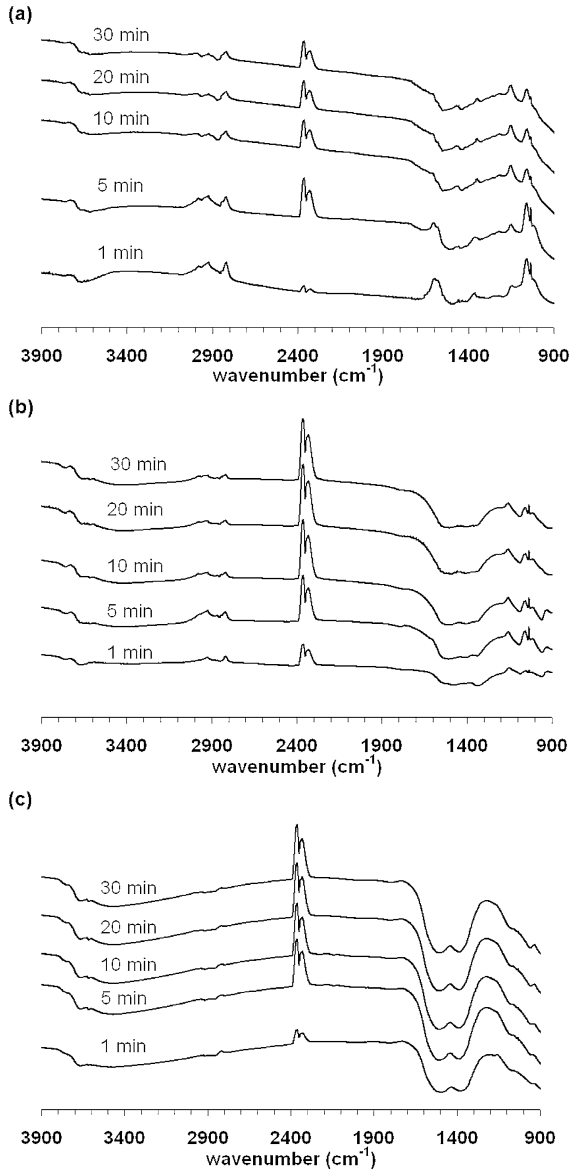


Fig. 16. DRIFTS spectra of in situ steam reforming of methanol over hydrogen prereduced samples (a) CZZ-433(550), (b) CZZ-433(350), and (c) CZZA-433:0.5.

periments. It should again be pointed out that CZZ-433(350) was also the only sample that performed the same with or without prereduction by hydrogen.

In the final series of experiments, the samples were prereduced with hydrogen before initiating the steam reforming reaction. In all of the samples, the intensities of the suggested intermediates were insignificant compared with the intensity of $CO_2$, as shown in Figs. 16a–16c. Taking into account the results just reported for nonreduced CZZ-433(350), it is apparent that the best-performing catalysts do not have a significant buildup of the intermediate species (or maybe spectator species) observed on unreduced CZZA-433:0.5 and CZZ-433(550) samples. In addition, the "activated" catalysts have a valley in the carbonate region and a surplus of hydroxides above the 3656 $cm^{-1}$ valley. After several hours of treatment, CZZ-433(550) catalyst did not have any significant differences in the DRIFTS spectra (not shown) compared with the spectra after 30 min of reaction.

There are several possible explanations for these observations. First, more active samples form more $CO_2$ as a product, so the $CO_2$ peak would be expected to be more intense, although probably not to the extent observed. If this were the case, then sintering effects could explain differences in Cu surface area and activity. Results from XPS after various treatments indicated a correlation between Cu surface area and activity; however, the differences were not as extreme as the activity differences. A second possibility is that different rate-limiting steps could be controlling the reaction on different catalysts. In this case, the buildup of intermediate species would be the result of a "bottleneck" effect on the less active catalysts. If the mechanism proceeded through the spillover of a species, then this could explain why samples with better Cu dispersion might have a different rate-controlling step. Third, despite the fact that the bulk CuO phase of all of the catalysts can be reduced by methanol, it is possible that part of the surface is being left in an inactive state for some samples treated with the reaction mixture and that the assumed intermediates are just bystander species that are building up on these inactive sites. Finally, it is possible that multiple steady states exist on these samples and that the state reached depends on the surface species present when the reaction is initiated. In the case of hydrogen-reduced samples, carbonates are cleaned from the sample and hydrogen is built up on the support, creating the most active catalyst. Only CZZ-433(350), with its high Cu surface area, appears to be able reach this state with or without prereduction with hydrogen, perhaps because of differences in surface composition, whereas the other samples remain in a less active steady state unless prereduced with hydrogen.

## 4. Conclusions

A series of catalysts for the methanol steam reforming reaction were found to have varying dependence of activity on pretreatment conditions. In general, characterization showed that the bulk CuO phase in all catalysts was reduced by the reactant mixture, similar to a hydrogen reduction. However, reduction with methanol caused additional sintering and loss of Cu surface area compared with reduction with hydrogen. If water was present in the feed, then the exothermicity of the reduction and the loss of Cu surface area during the reduction was less significant for all samples.

Evidence suggests that hydroxide and carbonates are removed from the surface of the catalysts during reduction with hydrogen. The removal of these species appears to be essential for better activity. The only sample that had identical activity with or without prereduction was also the only sample in which hydroxide and carbonate species were removed during reduction with methanol and water as well as

with hydrogen. Moreover, this sample had the least exothermic reduction and the highest mass loss during different reduction treatments. Several possibilities to explain these observations have been discussed; overall, these insights will contribute to a better understanding and design of catalytic systems for mobile methanol steam reforming to hydrogen.

## Acknowledgments

The authors gratefully acknowledge financial support from the National Science Foundation (grants DMR-0114098 and DGE-0221678).

## References

[1] R.F. Mann, J.C. Amphlett, B. Peppley, C.P. Thurgood, Int. J. Chem. Reactor Eng. 2 (2004) A5.
[2] C. Rhodes, G.J. Hutchings, A.M. Ward, Catal. Today 23 (1995) 43–58.
[3] M.S. Wainwright, D.L. Trimm, Catal. Today 23 (1995) 29–42.
[4] H.H. Kung, Catal. Rev.-Sci. Eng. 22 (1980) 235–259.
[5] Y. Nitta, O. Suwata, Y. Ikeda, Y. Okamoto, T. Imanaka, Catal. Lett. (1994) 345–354.
[6] M. Bowker, R.A. Hadden, H. Houghton, J.N.K. Hyland, K.C. Waugh, J. Catal. 109 (1988) 263–273.
[7] K.T. Jung, A.T. Bell, Catal. Lett. 80 (2002) 63–68.
[8] T. Fujitani, J. Nakamurs, Catal. Lett. 56 (1998) 119–124.
[9] S. Fujita, S. Moribe, Y. Kanamori, M. Kakudate, N. Takezawa, Appl. Catal. A: Gen. 207 (2001) 121–128.
[10] D. Duprez, J. Barbier, Z. Ferhat Hamida, M.M. Bettahar, Appl. Catal. 12 (1984) 219–225.
[11] D. Duprez, Z. Ferhat-Hamida, M.M. Bettahar, J. Catal. 124 (1990) 1–11.
[12] J.P. Breen, J.R.H. Ross, Catal. Today 51 (1999) 521–533.
[13] J.P. Breen, F.C. Meunier, J.R.H. Ross, Chem. Commun. (1999) 2247–2248.
[14] S. Velu, K. Suzuki, M. Okazaki, M.P. Kapoor, T. Osaki, F. Ohashi, J. Catal. 194 (2000) 373–384.
[15] X.R. Zhang, P. Shi, J. Zhao, M. Zhao, C. Liu, Fuel Proc. Technol. 83 (2003) 183–192.
[16] J. Agrell, H. Birgersson, M. Boutonnoet, I. Melian-Cabrera, R.M. Navarro, J.L.G. Fierro, J. Catal. 219 (2003) 389–403.
[17] P.H. Matter, D.J. Braden, U.S. Ozkan, J. Catal. 223 (2004) 340–351.
[18] A. Mastalir, B. Frank, A. Szizybalski, H. Soerijanto, A. Deshpande, M. Niederberger, R. Schomacker, R. Schlogl, T. Ressler, J. Catal. 230 (2005) 464–475.
[19] T.-J. Huang, S.-W. Wang, Appl. Catal. A: Gen. 24 (1986) 287–297.
[20] L. Alejo, R. Lago, M.A. Pena, J.L.G. Fierro, Appl. Catal. A: Gen. 162 (1997) 281–297.
[21] R.M. Navarro, M.A. Pena, J.L.G. Fierro, J. Catal. 212 (2002) 112–118.
[22] S. Velu, K. Suzuki, T. Osaki, Catal. Lett. 62 (1999) 159–167.
[23] T.L. Reitz, S. Ahmed, M. Krumpelt, R. Kumar, H.H. Kung, J. Mol. Catal. A: Chem. 162 (2000) 275–285.
[24] S. Velu, K. Suzuki, Top. Catal. 22 (2003) 235–244.
[25] B. Lindstrom, L.J. Pettersson, Int. J. Hydrogen En. 26 (2001) 923–933.
[26] R.O. Idem, N.N. Bakhshi, Ind. Eng. Chem. Res. 34 (1995) 1548–1557.
[27] S. Catillon, C. Louis, R. Rouget, Top. Catal. 30/31 (2004) 463–467.
[28] G. Fierro, M. Lo Jacono, M. Inversi, P. Porta, F. Cioci, R. Lavecchia, Appl. Catal. A: Gen. 137 (1996) 327–348.
[29] D. Bianchi, J.-L. Gass, M. Khalfallah, S.J. Teichner, Appl. Catal. A: Gen. 101 (1993) 297–315.
[30] I.A. Fisher, A.T. Bell, J. Catal. 178 (1998) 153–173.
[31] D. Bianchi, T. Chafik, M. Khalfallah, S.J. Teichner, Appl. Catal. A: Gen. 112 (1994) 219–235.
[32] D. Bianchi, T. Chafik, M. Khalfallah, S.J. Teichner, Appl. Catal. A: Gen. 123 (1995) 89–110.
[33] M.M. Gunter, T. Ressler, R.E. Jentoft, B. Bems, J. Catal. 203 (2001) 133–149.
[34] M.V. Twigg, M.S. Spencer, Top. Catal. 22 (2003) 191–203.
[35] A.J. Marchi, C.R. Apesteguia, Appl. Clay Sci. 13 (1998) 35–48.
[36] T.L. Reitz, P.L. Lee, K.F. Czaplewski, J.C. Lang, K.E. Popp, H.H. Kung, J. Catal. 199 (2001) 193–201.
[37] R.T. Figueiredo, A. Martinez-Arias, M.L. Granados, J.L.G. Fierro, J. Catal. 178 (1998) 146–152.
[38] Y. Okamoto, K. Fukino, T. Imanaka, S. Teranishi, J. Phys. Chem. 87 (1983) 3747–3754.
[39] J. Agrell, M. Boutonnoet, I. Melian-Cabrera, J.L.G. Fierro, Appl. Catal. A: Gen. 253 (2003) 201–211.
[40] F. Raimondi, K. Geissler, J. Wambach, A. Wokaun, Appl. Surf. Sci. 189 (2002) 59–71.
[41] S. Velu, K. Suzuki, C.S. Gopinath, H. Yoshida, T. Hattori, Phys. Chem. Chem. Phys. 4 (2002) 1990–1999.
[42] B.A. Peppley, J.C. Amphlett, L.M. Kearns, R.F. Mann, Appl. Catal. A: Gen. 179 (1999) 31–49.
[43] N. Nomura, T. Tagawa, S. Goto, Appl. Catal. A: Gen. 166 (1998) 321–326.
[44] N.-Y. Topsoe, H. Topsoe, J. Mol. Catal. A: Chem. 141 (1999) 95–105.
[45] S. Edwards, J. Phys. Chem. 89 (1985) 782.
[46] F. Boccuzzi, E. Borello, A. Zecchina, A. Bossi, M. Camia, J. Catal. 51 (1978) 150–159.
[47] G.J. Millar, C.H. Rochester, K.C. Waugh, J. Chem. Soc., Faraday Trans. 88 (1992) 1033–1039.
[48] C. Schild, A. Wokaun, A. Baiker, J. Mol. Catal. 63 (1990) 243–254.
[49] D. Bianchi, T. Chafik, M. Khalfallah, S.J. Teichner, Appl. Catal. A: Gen. 105 (1993) 223–249.
[50] A. Kudelski, B. Pettinger, Surf. Sci. 566–568 (2004) 1007–1011.
[51] C. Ammon, A. Bayer, G. Held, B. Richter, T. Schmidt, H.-P. Stienruck, Surf. Sci. 507–510 (2002) 845–850.
[52] J. Greeley, M. Mavrikakis, J. Catal. 208 (2002) 291–300.
[53] S. Sakong, A. Groß, J. Catal. 231 (2005) 420–429.
[54] I.E. Wachs, R.J. Madix, J. Catal. 53 (1978) 208–227.
[55] M. Bensitel, V. Moravek, J. Lamotte, O. Saur, J. Lavalley, Spectrochim. Acta 43A (1987) 1487–1491.